Acta Montanistica Slovaca
ISSN 1335-1788
actamont.tuke.sk

Relieving Pressure and Improving Permeability of Soft Coal at Top and Bottom by Hydraulic Cavitation

Shuren WANG[1], Guoji MA[2], Dingqi LI[3], Yunxing CAO[4] and Wenxue CHEN[5]*

Authors' affiliations and addresses:
[1] School of Civil Engineering, Henan Polytechnic University, Jiaozuo 454003, China
e-mail: shurenwang@hpu.edu.cn

[2] School of Civil Engineering, Henan Polytechnic University, Jiaozuo 454003, China
e-mail: 3204517695@qq.com

[3] School of Energy Science and Engineering, Henan Polytechnic University, Jiaozuo 454003, China
e-mail: lidingqi1979@163.com

[4] Institute of Resources and Environment, Henan Polytechnic University, Jiaozuo 454003, China
e-mail: yxcao17@126.com

[5] Department of Civil & Building Engineering, University of Sherbrooke, Sherbrooke J1K 2R1, Canada
e-mail: Wenxue.chen@usherbrooke.ca

***Correspondence:**
Shuren WANG, School of Civil Engineering, Henan Polytechnic University, Jiaozuo 454003, China; International Joint Research Laboratory of Henan Province for Underground Space Development and Disaster Prevention, Jiaozuo 454003, China
tel.: +86 15738529570
e-mail: shurenwang@hpu.edu.cn

Funding information:
Key Project of Natural Science Foundation of Henan Province (232300421134), First-Class Discipline Implementation of Safety Science and Engineering of Henan Province (AQ20230103), and National Scholarship Fund of China [2023].

Acknowledgement:
The authors would like to express their sincere gratitude to the editor and reviewers for their valuable comments, which have greatly improved this paper.

How to cite this article:
Wang, S.R., Ma, G.J., Li, D.Q., Cao, Y.X., and Chen, W.X. (2023). Relieving pressure and improving permeability of soft coal at top and bottom by hydraulic cavitation. *Acta Montanistica Slovaca*, Volume 28 (1), 157-178.

DOI:
https://doi.org/10.46544/AMS.v28i1.13

Abstract
For enhancing the effect of gas extraction, applying Wuyang Coal Mine in China as the engineering background, the technology of hydraulic cavitation at the top and bottom of soft coal (HCTBSC) with low permeability was put forward. FLAC^{3D} was utilized to build the calculation model, and Tecplot was employed to process data of the results, revealing the characteristics of stress variation in coal seam for different cavitation radius and different distribution forms of cavitation. The field test scheme of HCTBSC was determined to verify the simulation results. Results show that the effectiveness of stress relief (ESR) is controlled by the cavitation radius and cavitation distribution forms. The dimension of pressure relief emanates via the cavitation elongating outward with the cavitation radius, and the stress changes in the coal are different due to different cavitation distribution forms. The field test proves that the technology of HCTBSC is more effective in relieving pressure, increasing the productiveness of gas extraction, and decreasing the scourge of coal and gas protrusion. The obtained conclusions in this study provide guidance for the hydraulic cavitation application in soft coal.

Keywords
Low permeability, Soft coal, Pressure relief, Hydraulic cavitation, Improving permeability.

Introduction

Recently, with the development of coal mining, the coal resources in shallow layers have been exhausted. With the gradual increment of coal exploiting depth, the gas pressure and ground stress have also increased. The increasing coal depth triggers the progressive weakening of coal permeability, making it difficult for gas extraction and causing the high frequency of coal and gas protrusion (Xie et al., 2012; Soleimani et al., 2023; Kataoka et al., 2017; Wang et al., 2021a; Kim and Jeong, 2021; Chen et al., 2022).

The permeability of coal is an essential coefficient to measure the gas extraction capacity of a coal seam. In low-permeability coal, especially in soft coal, corresponding measures must be taken to promote pressure relief and improve the permeability of coal, improve gas extraction conditions, and realize the rapid deconstruction of working faces (Garagash et al., 2019; Yuan et al., 2015; Si et al., 2019; Jeffrey et al., 2015). At present, hydraulic measures (Ahamed et al., 2021; Vasyliev, 2019; Huang et al., 2013; Black, 2019; Lu et al., 2022; Ivakhnenko et al., 2017; Li et al., 2020) are usually utilized to relieve pressure and improve the permeability of coal. Different hydraulic ways produce different effects of depressurization on coal, coal and gas protrusion prevention and control, and subsequent coal roadway excavation and retrieval.

Thus, it is important to investigate the antireflection measures of coal, summarize and analyze the advantages and disadvantages of different antireflection measures, and provide technical guidance for gas extraction, relieving pressure and improving the permeability of coal.

State of the art

Making hydraulic cavitation in coal means that a high-pressure water jet is utilized to cut the coal around the borehole, and a wide territory of cavitation is formed in the coal. The coal adjacent to the cavity moves to the orientation of the borehole under the ground stress, and the old crevices among the coal are constantly enlarging and elongating. While a lot of new crevices are arising, which improves the permeability of the coal and the productiveness of gas extraction. Aimed at the problems of gas pre-drainage and low-drainage in deep coal, Gu and Wu (2021) investigated the impacts of gas drainage and crack enlargement in coal under different coal generation situations. Cao et al. (2021) derived the relationship between the effective gas drainage range and the hydraulic punching radius and gave the theoretical equation between the total gas drainage and the effective drainage radius. Hao et al. (2014) studied the gas drainage radius of hydraulic flushing and optimized the parameters of borehole arrangements. Zberovskyi et al. (2020) utilized the acoustic detection system to monitor the hydraulic impact disintegration effect of the outburst-prone coal in the development roadway. Wang et al. (2022) built a soft coal model with numerical software and evaluated the effect of hydraulic cavity pressure relief by down-seam and through-seam. Li and Teng (2021) analyzed the impact of drill hole spacing and hole diameter on gas compression, gas-containing capacity and coal permeability by numerical simulation, and they optimized the arrangement scheme of the bottom drainage roadway through the layer drilling. Liu et al. (2021) investigated the water jet laminar hydraulic punching technique for soft coal through experiments and numerical simulations and studied the laws of hydraulic punching jet branch number, gas-containing capacity and compression changes in coal. The hydraulic cavitation will form a large stress concentration region in the coal, which will bring safety hazards for the subsequent roadway excavation and coal retrieval.

Many scholars have sufficiently explored the mining of coal, utilized to promote pressure relief and improve the permeability of coal and increase the productiveness of gas extraction. Yang and Zhou (2022) experimentally investigated the force and failure characteristics of coal perturbed by coal mining with cyclic loading. Yan et al. (2018) analyzed the fracture development zone of coal under the impact of mining and revealed that the distribution range moved forward as the working face advanced. Liu et al. (2009, 2014) found that after performing ultra-thin coal mining, the ground stress in the sheltered coal was reduced, and the deformation of the coal led to improved permeability and enhanced the productiveness of gas drainage. Cheng et al. (2018) took the soft rock layer as the conserved stratum mining and used the numerical method to study the mechanism of relieving pressure and improving the permeability of coal after coal mining. Li (2014) investigated the stress, permeability coefficient, and productiveness of gas drainage within the coal after thin coal seam mining in Yi'an mine, China. Yao et al. (2016) illustrated the impacts of the effectiveness of stress relief on the overlying coal stress, gas pressure, and coal permeability, and they analyzed the influence of coal mining and gas drainage on coal gas transport. Jiang et al. (2019) proposed an anti-scouring scheme for local protective layer mining and analyzed the mechanism of anti-scouring and large deformation hazard by numerical analysis method. The protective seam mining of sheltered coal effectively relieves pressure and reduces stress concentration in the coal due to cavity creation, but the protective seam mining cannot be applied in coal that does not have a protective seam.

To obtain a better effect of relieving pressure and improving permeability in coal, some scholars have combined two or more measures of relieving pressure and improving the permeability of coal. Wei et al. (2021) proposed a method that combined hydraulic slotting and liquid CO_2 injection to increase the permeability of coal and strengthen gas drainage productiveness. Xu et al. (2021) developed a new permeability enhancement technique

of "hydraulic flushing plus air cannon explosion" for vulnerable low-permeability coal, and they found the effect of different explosion times in the borehole after flushing on the permeability and the productiveness of gas drainage from the coal. Li et al. (2021) proposed the joint penetration technique of hydraulic flushing and deep hole pre-splitting bursting. They analyzed the mechanism of this technique and studied the stress allocation and expansion rhythmical of explosive crevices in coal under diverse clearance between the detonation hole and the controlled retrieval hole. These investigations show that the combination of two or more pressure relief measures has markedly improved the productiveness of gas extraction, but few scholars have discussed the ESR of coal after the combination of protective strata mining and hydraulic cavitation measures. Therefore, it is necessary to investigate the combination of different pressure release techniques to explore more appropriate pressure relief and gas drainage measures for coal.

While other scholars have performed lots of research on coal hydraulic cavitation, providing theoretical guidance for coal mine construction and obtaining rich scientific outcomes. However, regarding the coal that is suitable as a protection layer for mining, and at the same time avoiding the stress centralization generated by the cavity creation in the coal, ensuring the smooth excavation of the roadway, it is necessary to adopt a more suitable method to promote relieving pressure and improving permeability of coal and improve the gas resolving rate and gas drainage effect. Stem from a previous investigation, this study proposed the technology of HCTBSC, in which the 0.5 m-thick coal body at the top and bottom of the coal (TBC) is used as the "protective layer" of the coal, and the hydraulic cavitation was carried out at this layer. A model was built by FLAC^{3D} to investigate the effects of cavitation radius and cavitation distribution forms on the stress changes of the coal. The practicality of HCTBSC was verified by the field tests.

The rest of this study is organized as follows. The relevant background and the research methods are described in the section Materials and Methods. Then the results and discussion are given, and finally, the conclusions are summarized.

Materials and Methods

Engineering Background

The drilling interval type hydraulic cavity was adopted in the Wuyang coal mine in China to relieve pressure and increase penetration technology in the 80-0305 bottom pumping lane to increase the productivity of gas drainage and the excavation speed of the 8005 return air lane and 8003 transport lane. 80-0305 bottom pumping lane drilling design and final hole plan are shown in Fig. 1. The result of field application shows that this technology has greatly ascended the productiveness of gas drainage in coal roadway excavation, but there are still some problems to be optimized:

(1) Low construction efficiency, the volume of coal output from hydraulic cavity making is large, the construction time of a single cavity of the borehole was prolonged, and the construction efficiency of the borehole is low.

(2) The dimension of stress relief (DSR) of hydraulic cavitation is controlled by the structure of the coal body. The stress centralization zone is easily formed around the hole after hydraulic cavitation.

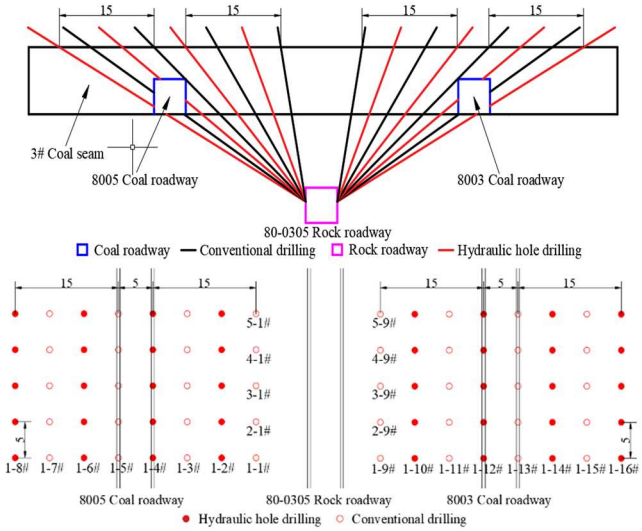

(a) Drilling design drawing (unit: m) *(b) Layout plan of boreholes termination (unit: m)*

Fig. 1. Drill hole design and layout of final holes.

In view of the problems in the Wuyang coal mine, the technology of HCTBSC was proposed. The coal below the apical plate and above the baseplate of the coal was selected as the hydraulic cavitation layer, using directional water jets for hydraulic cavitation along the top and bottom plates, which can improve the efficiency of relieving pressure and improving permeability in coal, to effectuate the efficient mining of low-permeability soft coal.

Numerical simulation analysis

The computational model. FLAC^{3D} numerical simulation technique was implemented to observe the stress changes after HCTBSC and in the middle of the coal under different cavitation radii (Pezdevsek et al., 2022; Wang et al., 2021b; Godec et al., 2021). A multi-borehole model was established, which analyzed the interaction impact of stress changes among boreholes with different cavitation radii and different cavitation distribution forms, guiding the construction of actual through-seam hydraulic cavitation boreholes.

According to the Wuyang coal mine, we built a single-hole model of 15 m × 15 m × 14 m within FLAC^{3D} (Long et al., 2021; Kolomiets et al., 2021; Wang et al., 2021). The model was segregated into 3 strata; the top-down order is sandy mudstone (apical plate), primary hard coal, and sandy mudstone (bottom plate). For example, the model clustering and cavitation schematic is shown in Fig. 2 with the cavitation radius R = 0.6 m.

Model parameter settings. After the modelling is completed, assigning the mechanical parameters to the coal rock body in the model is indispensable. According to the mechanical parameter information of coal rock in the Wuyang coal mine, the model was divided into three layers: coal bottom, primary coal and coal top; the corresponding thicknesses were 4.7 m, 5.54 m, and 3.76 m. The thicknesses of coal rock layers and their mechanical parameters are shown in Table 1.

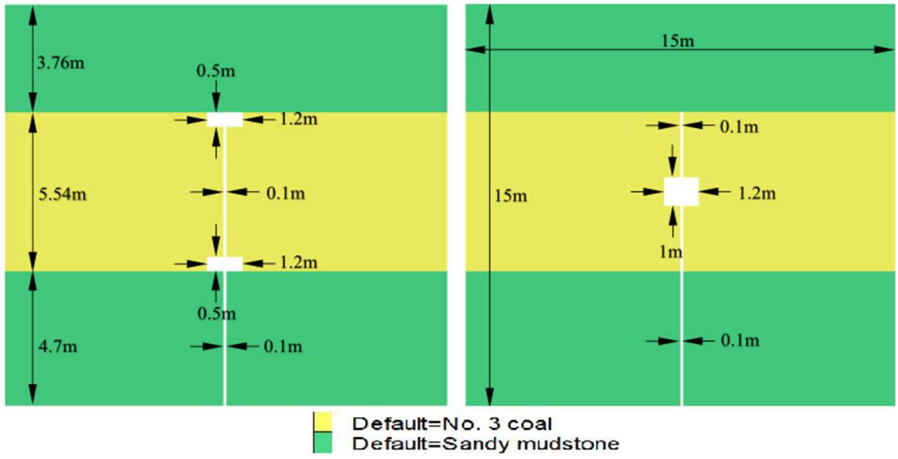

Fig. 2. Model grouping and hydraulic cavitation diagram.

Tab. 1. Mechanical parameters of coal strata in Wuyang Coal Mine.

Name	Thickness [m]	Density [kg/m^3]	Tensile strength [MPa]	Cohesion strength [MPa]	Bulk modulus [GPa]	Poisson' ratio	Internal friction angle [°]
Sandy mudstone	3.76	2500	0.8	7.0	4.01	0.23	24
No. 3 coal	5.54	1350	0.64	1.4	1.19	0.28	16
Sandy mudstone	4.70	2500	0.8	7.0	4.01	0.23	24

HCTBSC was performed in the coal; the cavitation radius R was separately interposed to 0.4 m, 0.6 m, and 0.8 m, respectively. The cavitation length was 0.5 m thickness of coal of TBC, the radius of the borehole in the baseplate, and the primary coal where the cavitation was not performed was 0.05 m. Around the model was roller support; the underneath was fastening enslavement; the upper was the free boundary. Considering the dead weight of the overlying stratum, applying the normal stress of 15.1 MPa to the upper apex of the model, and the normal stress was calculated in Eq. (1). The stress in the horizontal direction coincides with the stress in the vertical orientation, the coal rock body was in the hydrostatic stress state, the modelling was completed to calculate the model and analyze the calculation results.

$$\sigma_v = \gamma H \tag{1}$$

where, σ_v is the normal stress of coal, MPa. γ is the bulk density of overburdened rock stratum, 25 kN/m^3. H is the embedded depth of coal, m.

Design of field experiments. According to the construction of the 8000 bottom pumping lane in the Wuyang coal mine, the segment of 500-550 m was selected from the lane entrance in the lane as the trial area. There were 8 sets of boreholes in the left gang of the roadway in the trial zone; the spacing among each set of boreholes was

5 m, each set of boreholes was arranged in 2 columns, and the spacing between columns was 2.5 m. Each column is arranged in two rows; the spacing between rows was 0.3 m, the lower row of boreholes was 2.3 m above the bottom of the roadway, the upper row of boreholes was 0.3 m below the top of the roadway, and each row was arranged with 4 boreholes. The design length of the boreholes varied greatly due to the angle of the borehole construction, and the depth of the boreholes was generally between 50 and 90 m. The schematic opening and final arrangement of HCTBSC are shown in Fig. 3. After the completion of the drilling construction, the borehole was sealed, and the gas drainage consistency of a piece borehole was monitored and recorded regularly so as to compare with the gas extraction consistency of the borehole interval type middle coal hydraulic cavern used in Wuyang coal mine.

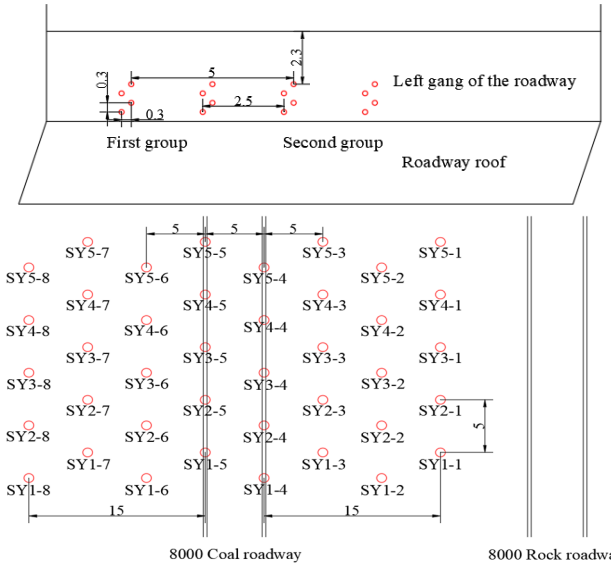

(a) Diagram of opening borehole position (unit: m) *(b) Final hole layout (unit: m)*

Fig. 3. Drilling design and final hole layout.

The borehole was drilled to 0.5 m inside the apical plate of the coal; hydraulic cavitation was made below the apical plate and above the baseplate of the coal with 0.5 m thickness during the retreating process. The location of the hydraulic cavitation in the coal is shown in Fig. 4. When the drill pipe was retired to the hydraulic cavitation position. It was necessary to increase the water pressure of the branch water pumping truck to 18-22 MPa for cavitation; the drill pipe speed should be kept at about 120-180 rad/min during cavitation. It should be recorded in detail during the cavitation process, with 0.5 m³ of coal output per cavitation as the accepted standard, ensuring that the cavitation operation was stopped when the borehole returns clear water or no obvious coal slag or coal chips. After the cavity making was completed, all the drill pipes would be withdrawn, the borehole sealing and gas drainage were carried out, and the gas drainage consistency could be monitored regularly.

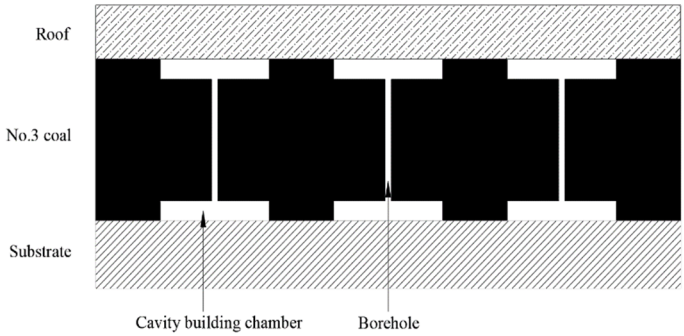

Fig. 4. Diagram of hydraulic cavitation of coal.

Results and Discussion

Principal stress analysis of HCTBSC

Single-hole principal stress analysis of HCTBSC. After HCTBSC is completed, the maximum and minimum principal stress allocations within the coal are shown in Fig. 5. The stress of the coal adjoins the

cavitation chamber and generates a secondary distribution. With the prolongation of time, the stress in the coal gradually releases. The coal body in the primary coal expands and deforms adjacent to the cavitation chamber. The length and width of the old fissures in the coal further expand while a lot of new crevices arise inside the coal. The perviousness of the coal is improved, and the gas resolving rate is increased. The gas in the coal is gradually extracted and finally reaches the goal of relieving pressure and increasing permeability.

In Fig. 5, with the increment of cavitation radius, the DSR in the native coal gradually enlarges. When the cavitation radius of TBC is 0.4 m, a dumbbell-like DSR is generated in the coal, and the vertical distance is 1.5 m between the edge of the stress area of less than 14 MPa in the DSR and the center axis of the borehole. With the gradual enlarging of the cavitation radius, the area is gradually extended to two-side of the borehole and alongside the vertical orientation of the coal with the cavern chamber as the center, the DSR and tensile stress are more obvious, while the DSR is gradually transformed the dumbbell-shaped into an hourglass shape. When the increment of cavitation radius to 0.8 m, the hourglass pressure area becomes more obvious. The vertical distance is 2.4 m between the edge of the stress area, less than 14 MPa in the DSR, and the central axis of the borehole. Regarding the maximum principal stress, the stress centralization zone is mostly concentrated around the cavity-making chamber of TBC and on two-side of the borehole. There is no large-scale stress centralization zone in the coal, which has less influence on the subsequent roadway excavation.

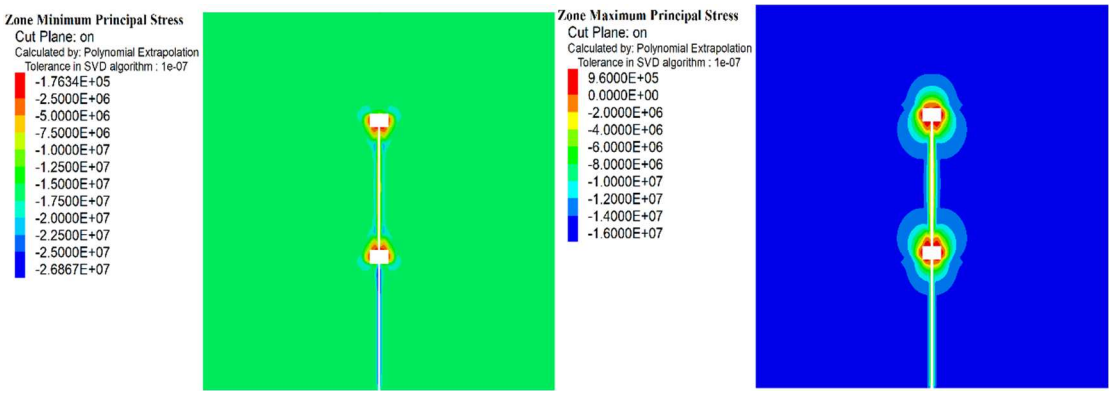

(a) R=0.4 m

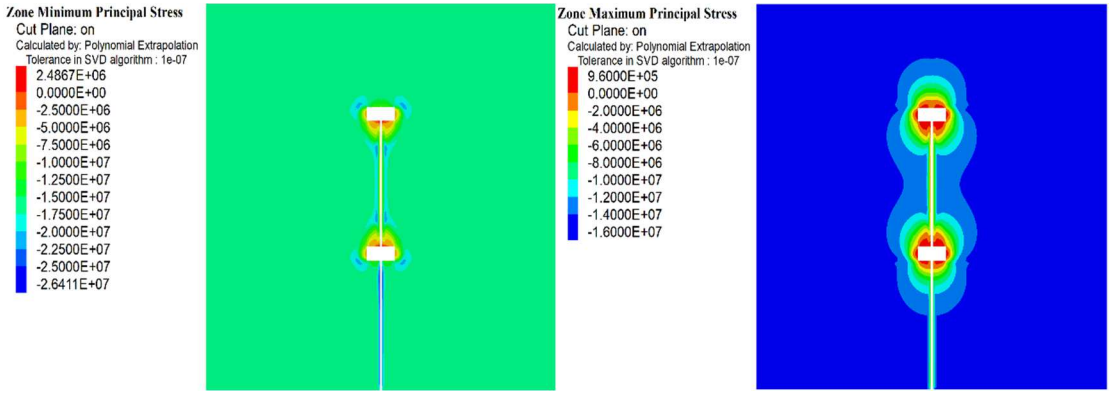

(b) R=0.6 m

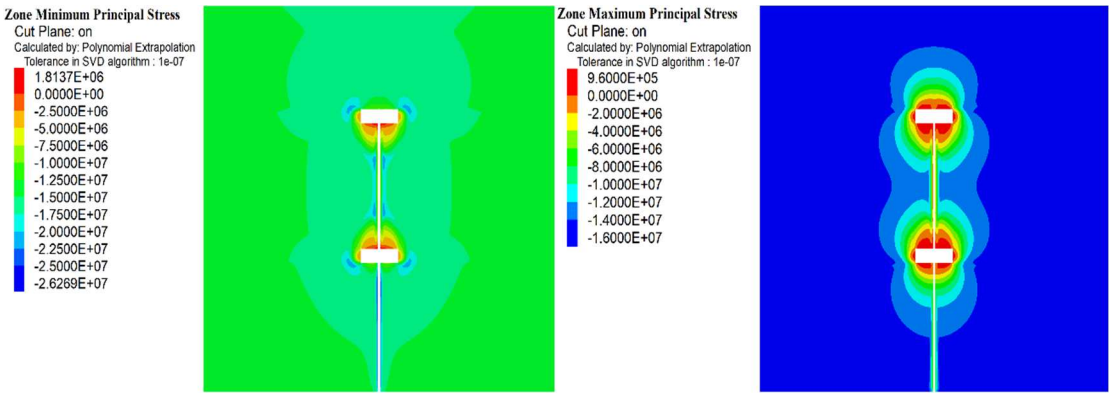

(c) R=0.8 m

Fig. 5. Single-hole stress variation of HCTBSC.

HCTBSC causes stress perturbation of different degrees in the whole coal area, and the minimum principal stress changes are the most obvious. The different ESR is generated in the area of the borehole and around the cavitation chamber, the adequate DSR is the coal nearby the cavitation chamber, and the ESR gradually decreases as the distance from the cavitation chamber increases. As for the maximum principal stress, the adequate zone for relieving pressure in the coal is the coal adjacent to the cavitation chamber, which is basically the same as the minimum principal stress. While the stress centralization zone mostly exists around the cavern chamber of TBC and two-side of the borehole.

Multi-hole principal stress analysis of HCTBSC. Based on the single-hole numerical model, a numerical multi-hole model of HCTBSC was built to analyze the stress allocation and the ESR of coal under the joint interaction of boreholes. The borehole spacing was fixed at 5 m to compare the ESR when the cavitation radius of TBC was separately interposed to 0.4 m, 0.6 m, and 0.8 m. The simulation results are shown in Fig. 6.

In Fig. 6, when the cavitation radius is 0.4 m, the generated stress disturbance is small by cavitation in each borehole; the ESR in the coal is weak. With the cavitation radius enlarging from 0.4 m to 0.6 m, the DSR generated by cavitation expands outward, and the DSR of the coal is approximate to a dumbbell shape by cavitation further extending to two-side of the borehole and alongside the vertical orientation.

When the increment of the cavitation radius reaches 0.8 m, the DSR further extends outward, and the DSR of the coal generated by the two cavitation holes is interconnected at the lower boundary of the roof cavitation chamber and the upper boundary of the bottom cavitation chamber. With the increment of cavitation radius, the DSR expands from TBC to the middle of the coal. There is an oval area with a poor pressure relief effect between two adjacent boreholes in the coal. As for the maximum principal stress, the stress concentration phenomenon in the coal is approximate to the single borehole coal top-bottom hydraulic cavitation, which is mostly concentrated around the cavitation chamber and two-side of the borehole.

When the borehole spacing is certain, as the increment of cavitation radius, the DSR in the coal develops to two-side of the borehole and alongside the vertical orientation of the coal until the DSR is connected between the adjacent boreholes, which causes a certain scope of stress turbulence to the whole coal area. The whole pressure discharge area with a better pressure discharge effect is formed in the coal, where the minimum principal stress change is the most pronounced. Therefore, being carrying out HCTBSC, we can consider increasing the cavitation radius to promote the pressure relief area to expand further outward and make the coal achieve a better pressure relief effect. But at the same time, we should also consider the influence of construction efficiency on the overall borehole construction.

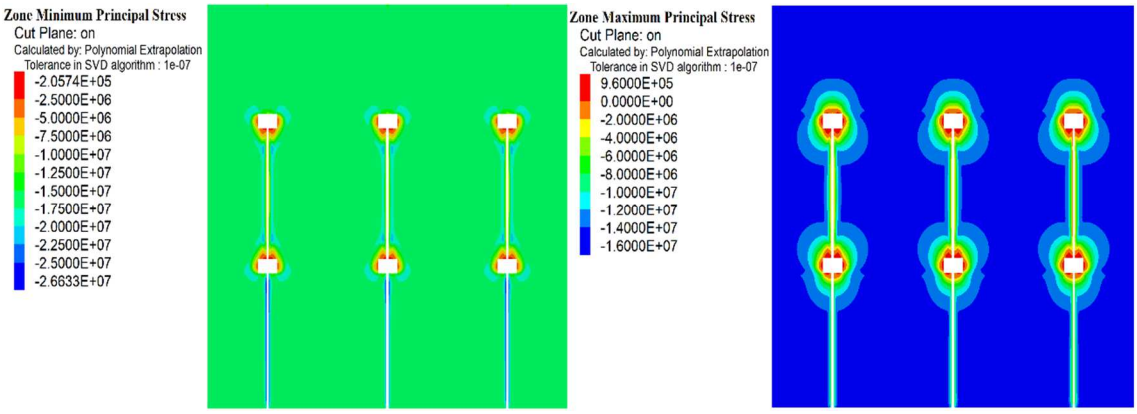

(a) R=0.4 m

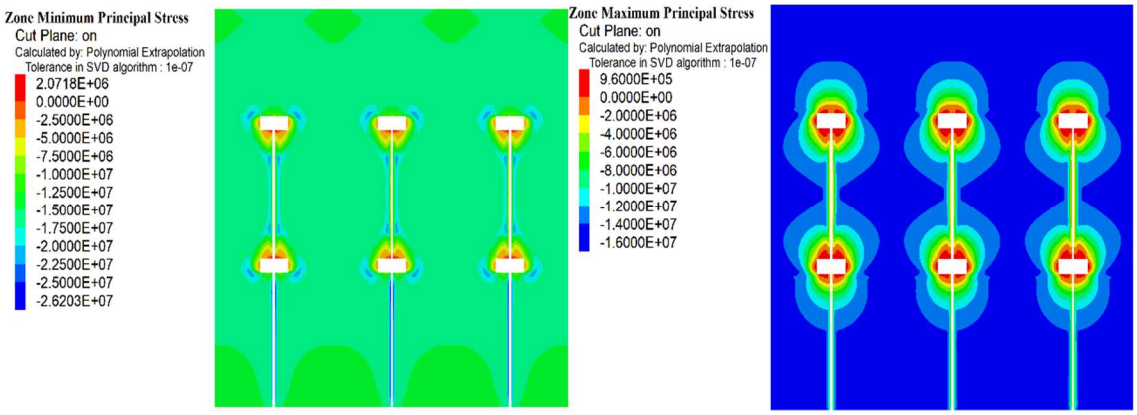

(b) R=0.6 m

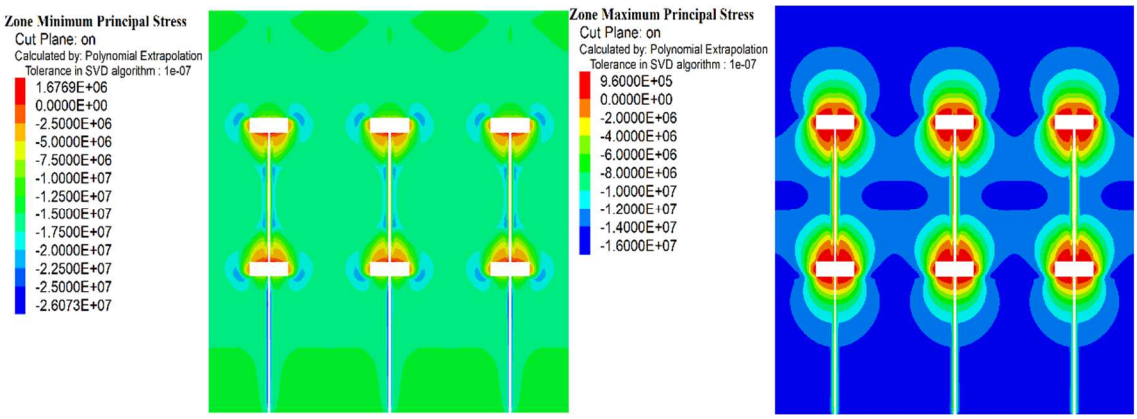

(c) R=0.8 m

Fig. 6. Porous stress variation of HCTBSC.

Principal stress analysis of hydraulic cavitation in the middle of soft coal (HCMSC)

To compare with the ESR of HCTBSC, the stress change of HCMSC was simulated and analyzed. After HCMSC is completed, the maximum and minimum principal stress allocation in the coal is shown in Fig. 7.

In Fig. 7, as the increase of cavitation radius, the DSR in the native coal gradually increases. When the radius of hydraulic cavitation is 0.4 m, the DSR is formed in the middle of the coal with the cavitation chamber as the center in an approximate circle. The vertical distance is 2.1 m between the edge of the stress area of less than 14 MPa in the DSR and the center axis of the borehole. With the increment of the cavitation radius, the area is expanded to the two-side and TBC with an approximately circular shape; the ESR gradually decreases with the increment of the distance to the cavitation chamber. When the increment of cavitation radius to 0.8 m, the DSR becomes more obvious in the coal, and the vertical distance is 3.2 m between the edge of the stress area less than 14 MPa in the DSR and the central axis of the borehole. The DSR basically covers the overall coal. As for the maximum principal stress, after HCMSC is completed, an inconspicuous stress concentration area is visible around the cavitation chamber, which will create certain safety hazards for the subsequent roadway excavation.

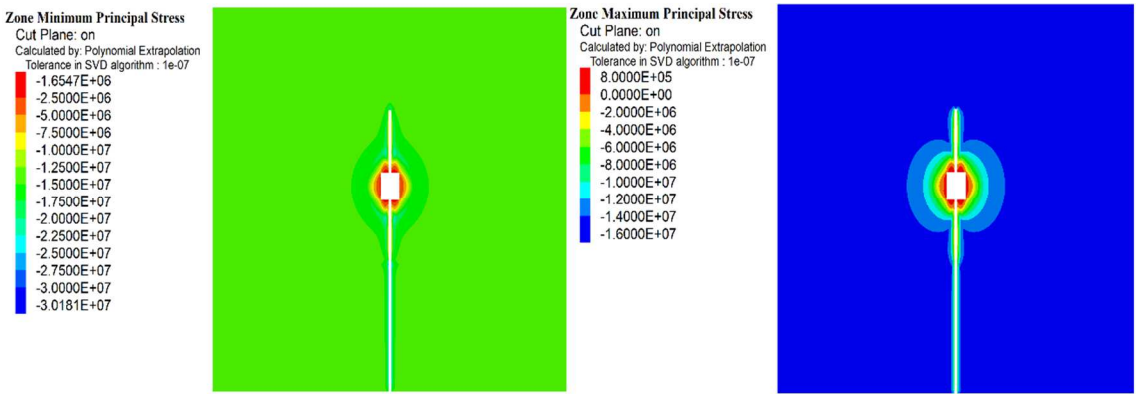

(a) R=0.4 m

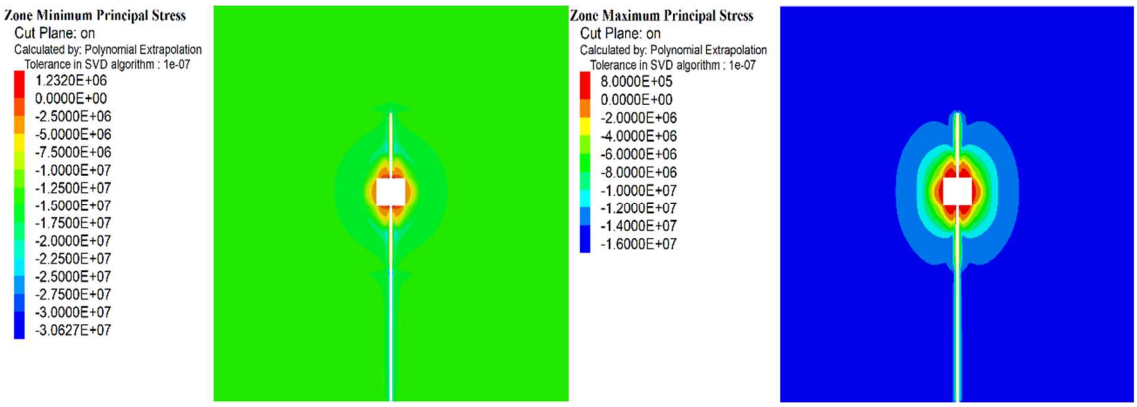

(b) R=0.6 m

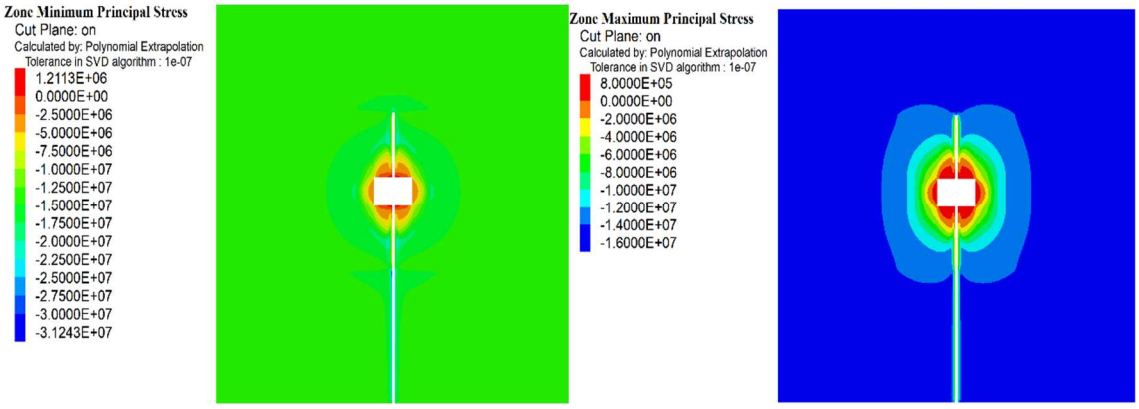

(c) R=0.8 m

Fig. 7. Single-hole stress variation of HCMSC.

After the completion of hydraulic cavitation, an approximately circular pressure relief area centred on the cavitation chamber is formed in the coal. The DSR extends outward as the cavitation radius increases; the ESR is most effective adjacent to the cavitation chamber, and the ESR gradually decreases with the increment of distance. As for the maximum principal stress cloud, there is no obvious stress concentration area around the cavitation chamber.

Multi-hole principal stress analysis of HCMSC. To investigate the interaction effect between the holes of HCMSC, a multi-hole model of HCMSC was built based on the single-hole model. The distance between the boreholes was fixed at 5 m, simulating and analyzing the ESR of coal with cavitation radius was separately interposed to 0.4 m, 0.6 m and 0.8 m. The related results are shown in Fig. 8.

In Fig. 8, when the cavitation radius is 0.4 m, the DSR is interconnected on two-side of the cavitation chamber, and the ESR of the coal is poor. As the cavitation radius augments from 0.4 m to 0.8 m, the DSR is further superimposed on two-side of the cavitation chamber; the DSR also extends to TBC, following the vertical orientation of the coal. The adequate pressure relief region is the coal adjacent to the cavitation chamber; the ESR is the best, and the DSR basically overspreads the integral coal. As for the maximum principal stress, a stress centralization zone is formed in the coal adjacent to the cavitation chamber after the completion of hydraulic cavitation. With the increase of cavitation radius, the stress centralization phenomenon becomes more obvious. When the increment of cavitation radius to 0.8 m, the stress centralization zone is interconnected at the residual coal body between the two cavitation chambers.

When the borehole spacing is certain, as the increase of cavitation radius, the ESR produced by HCMSC increases, and the connected area of the DSR in the coal gradually expands. The whole coal area is disturbed to different degrees. When the increment of cavitation radius to 0.8 m, the DSR overspreads the integral coal; the ESR produced by the cavitation is the most significant in the middle of the coal.

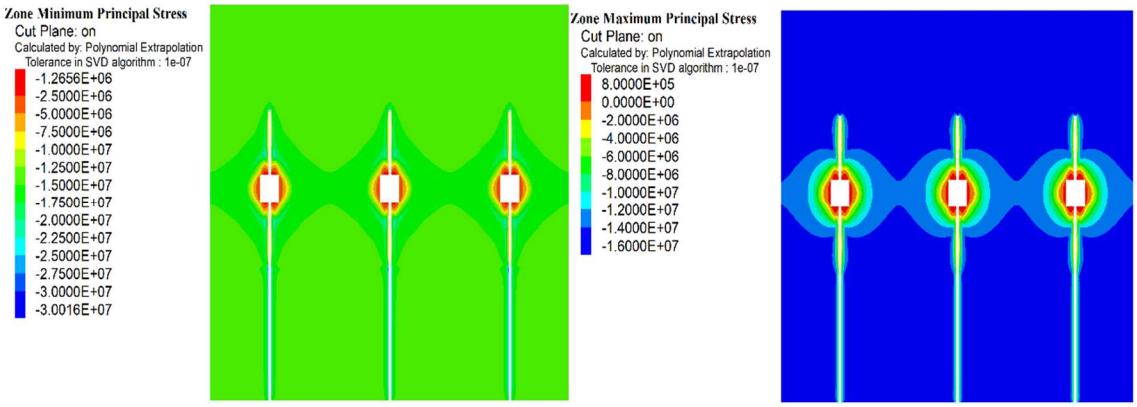

(a) R=0.4 m

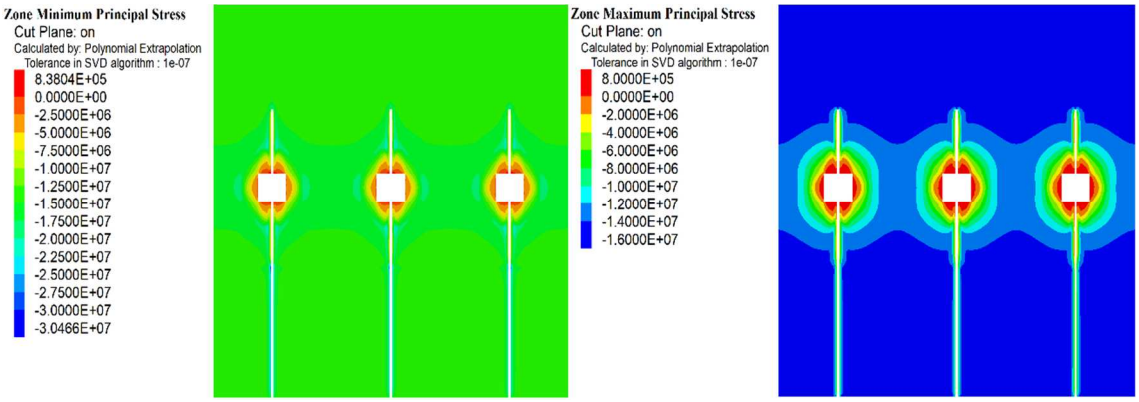

(b) R=0.6 m

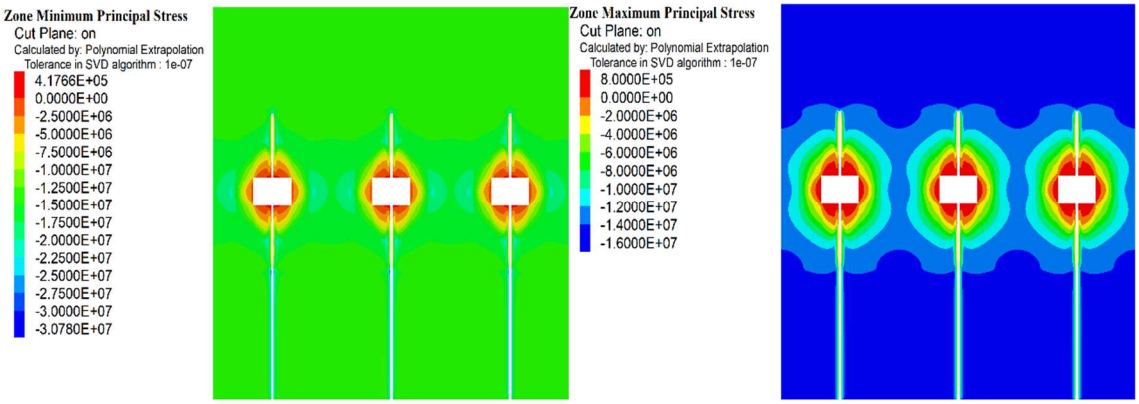

(c) R=0.8 m

Fig. 8. Porous stress variation of HCMSC.

Principal stress analysis of the combined hydraulic cavitation (CHC)**.** The stress perturbation effects from different cavitation distribution forms are also different. Combining the above two distribution forms of hydraulic cavitation, the stress changes were analyzed in the coal under different cavitation radius conditions of combined hydraulic cavitation by numerical simulation. The distance between the boreholes was fixed at 5 m, comparing and analyzing the ESR of the coal with cavitation radius separately interposed to 0.4 m, 0.6 m and 0.8 m. The simulation results are shown in Fig. 9.

In Fig. 9, when the radius of cavitation is 0.4 m, the stress perturbation of minimum principal between the boreholes of combined hydraulic cavitation is smaller; the smaller size of the cavitation chamber leads to weaker whole coal pressure relief. When the increment of cavitation radius to 0.6 m, the DSR increases significantly. The pressure relief area is first connected to the four corners of the DSR in the middle cavitation chamber and the DSR in the top and bottom cavitation chambers on two-side. When the increment of cavitation radius to 0.8 m, the scope of corner connection is larger. The DSR of the cavitation at the top and bottom expand and connect to the middle of the coal along the normal orientation; the ESR of the coal is better. As for the maximum principal stress, after the completion of the CHC, a stress concentration zone is generated in the coal body adjacent to the cavitation chamber; the stress concentration phenomenon generated by the CHC is a collection of the previously mentioned two cavitation measures.

When the borehole spacing is certain, as the increase of cavitation radius, the ESR of coal produced by CHC gradually increases, the stress turbulence range emerged by single-hole hydraulic cavitation is interconnected, and the minimum principal stress value of the whole coal is reduced.

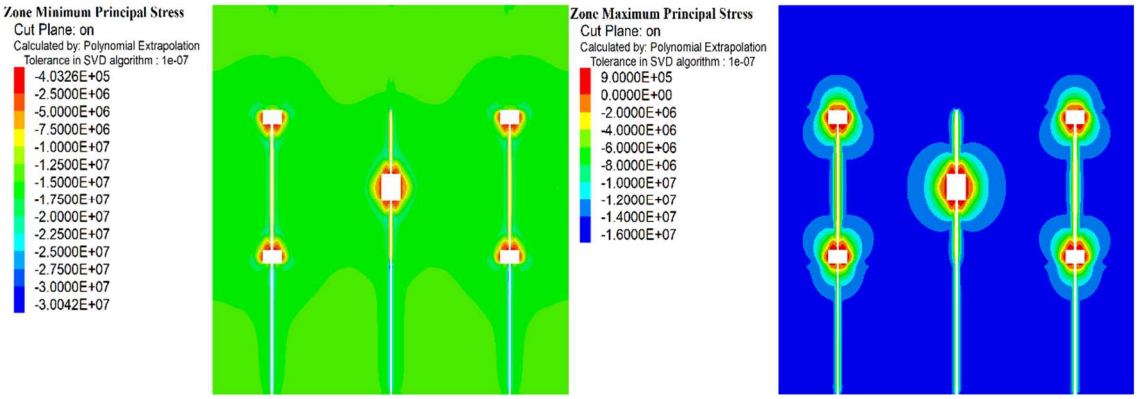

(a) R=0.4 m

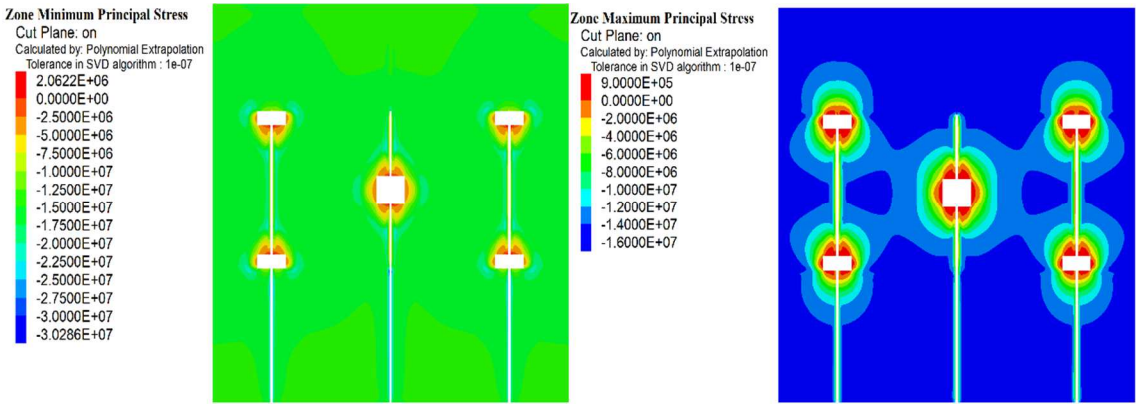

(b) R=0.6 m

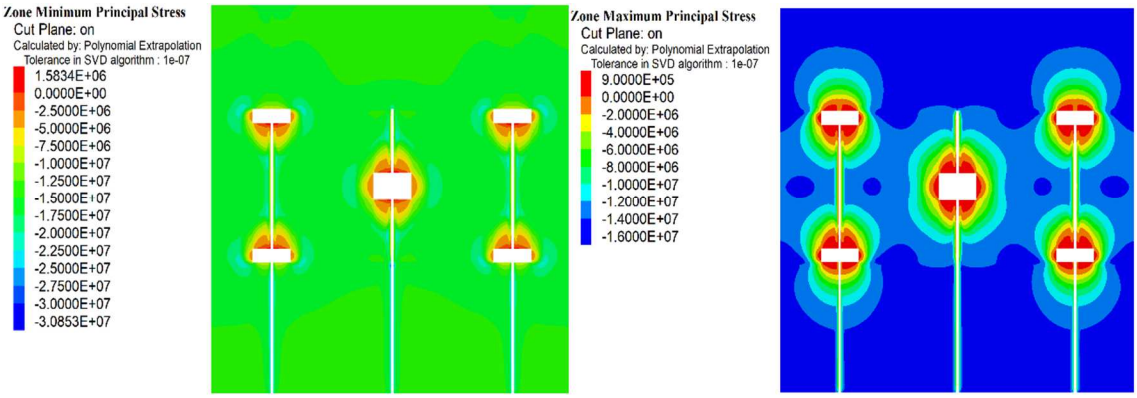

(c) R=0.8 m

Fig. 9. Stress variation of CHC.

Comparison of the ESR about porous hydraulic cavitation

To visually analyze the coal stress of the above multi-hole cavitation measures, the calculation results were sliced and processed using Tecplot software, and the stresses in the coal body were extracted at the locations of model height (y-axis) h = 4.95 m, h = 7.47 m and h = 9.99 m, respectively. The layout of the monitoring lines is shown in Fig. 10.

Compare the ESR of different cavitation radii. In Fig. 11, the stress allocation curves of the coal for the three cavitation measures with different cavitation radii. A set of curves in which the upper side is the minimum principal stress allocation curve, and the lower side is the maximum principal stress allocation curve. As the radius of the cavern increases, the minimum principal stress relief range gradually increases in the coal; the stress decreases at the uncavitated locations due to the ESR of cavitation. For the maximum principal stress, as the cavitation radius increases, the maximum principal stress in the coal adjacent to the cavitation chamber also increases.

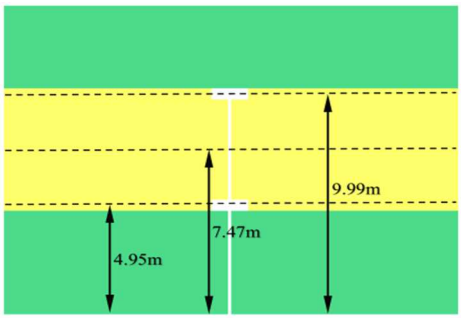

Fig. 10. Arrangement of stress monitoring line.

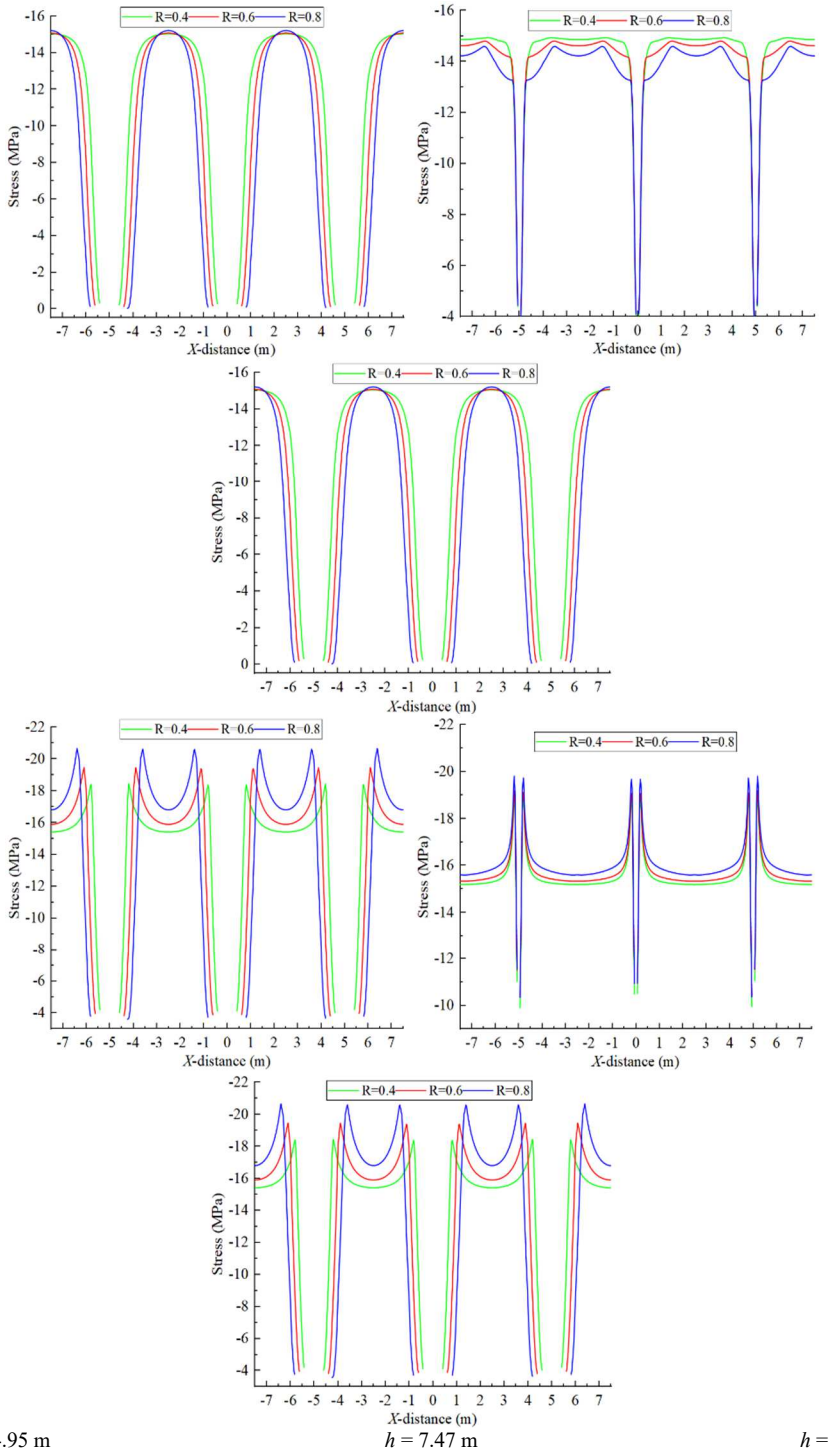

h = 4.95 m h = 7.47 m h = 9.99 m

(a) HCTBSC

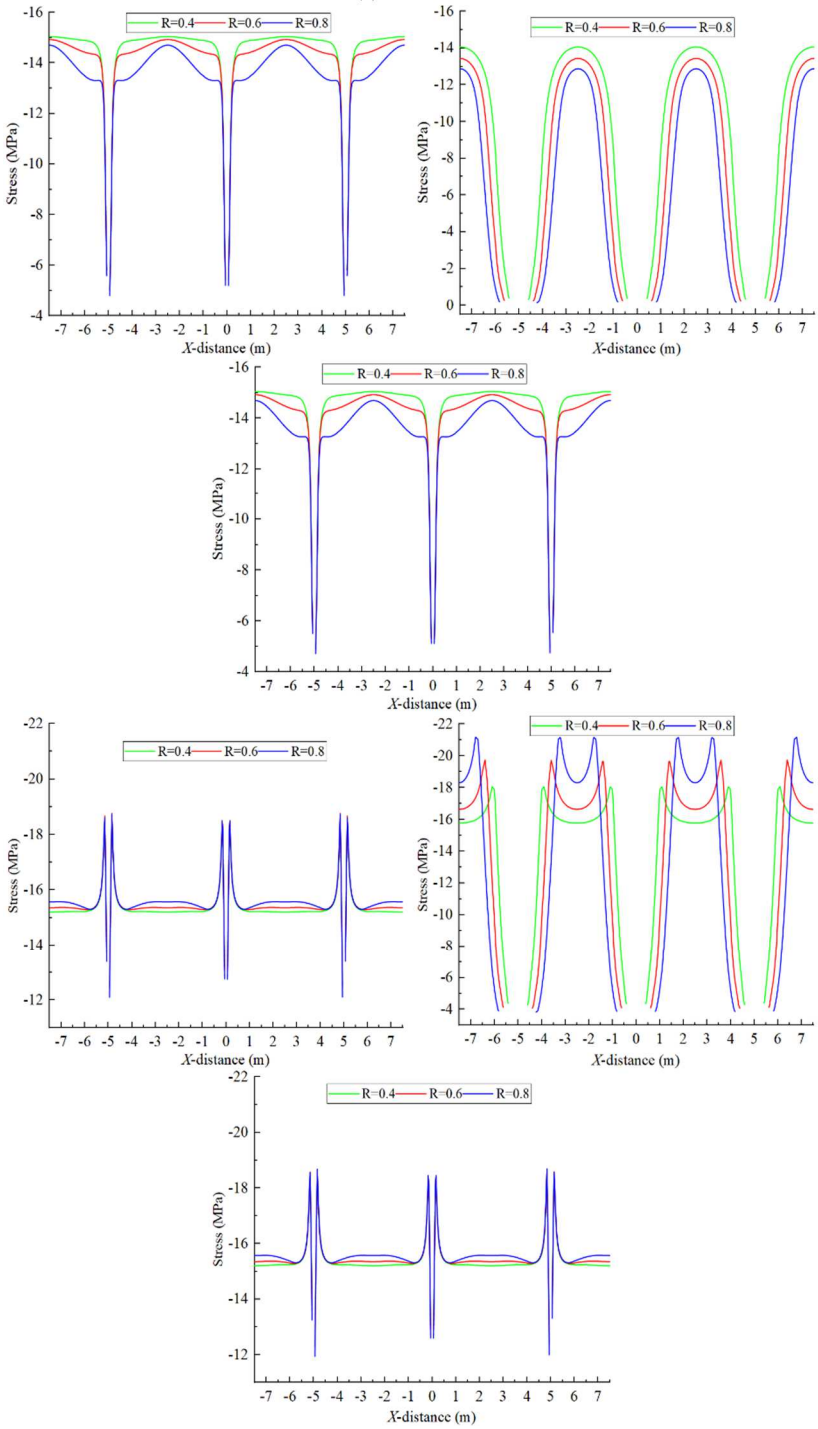

h = 4.95 m h = 7.47 m h = 9.99 m

(b) HCMSC

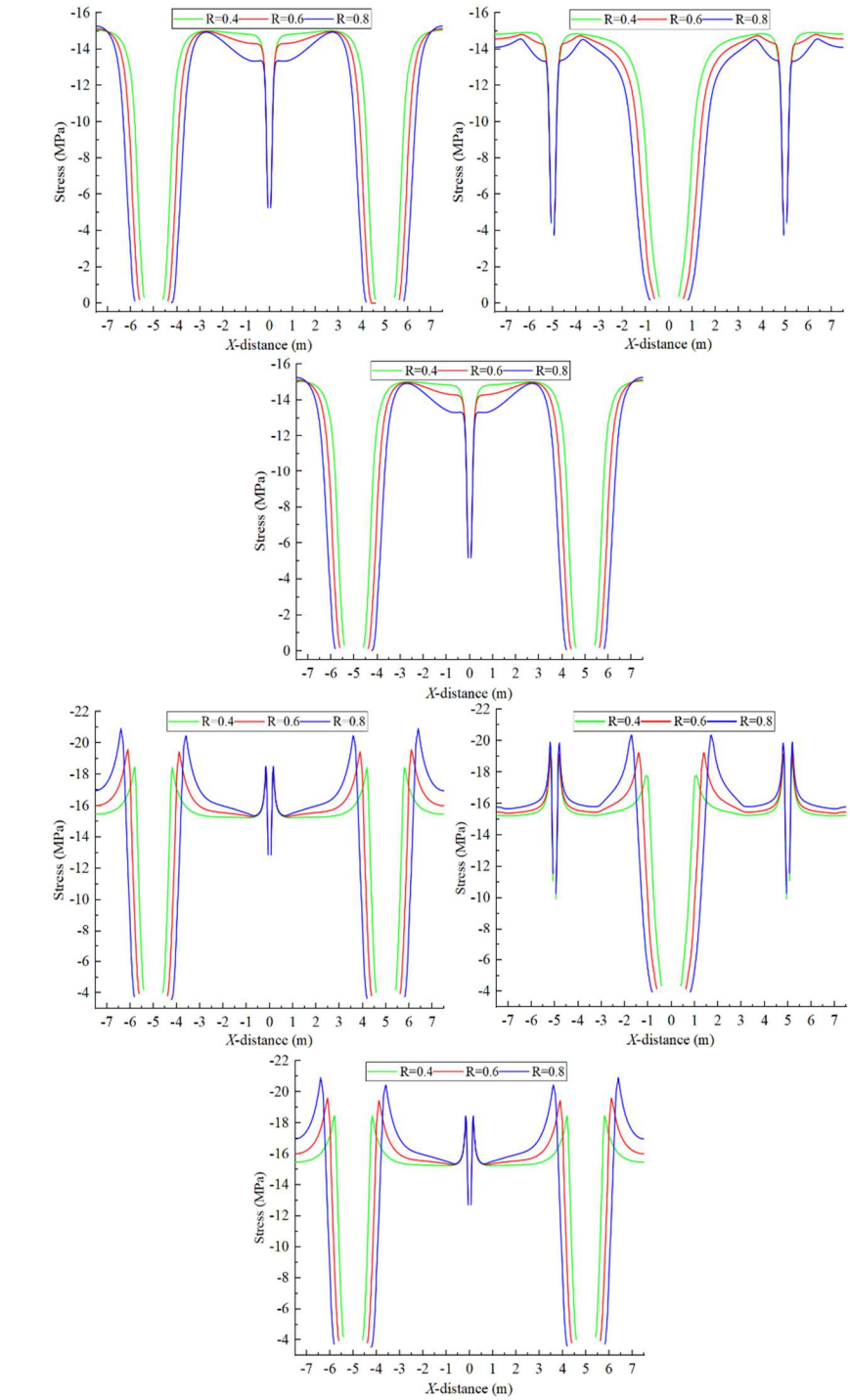

h = 4.95 m h = 7.47 m h = 9.99 m

(c) CHC

Fig. 11. Stress allocation curve with different cavitation radius.

Compare the ESR of different cavitation distribution forms. In Fig. 12, the stress allocation curves of the coal for the three cavitation measures with different forms of cavitation distribution. A set of curves in which the upper side is the minimum principal stress allocation curve, and the lower side is the maximum principal stress allocation curve. When the borehole spacing is certain, as the cavitation radius increases, the coal's ESR increases, and the minimum principal stress value decreases. As for the maximum principal stress value, as the radius of cavitation augments, the maximum principal stress value increases, which is at a certain borehole spacing. Under the same overlying rock pressure, the amount of residual coal between cavitation chambers becomes narrower due to the increase of cavitation radius, leading to stress concentration in the residual coal between cavitation chambers.

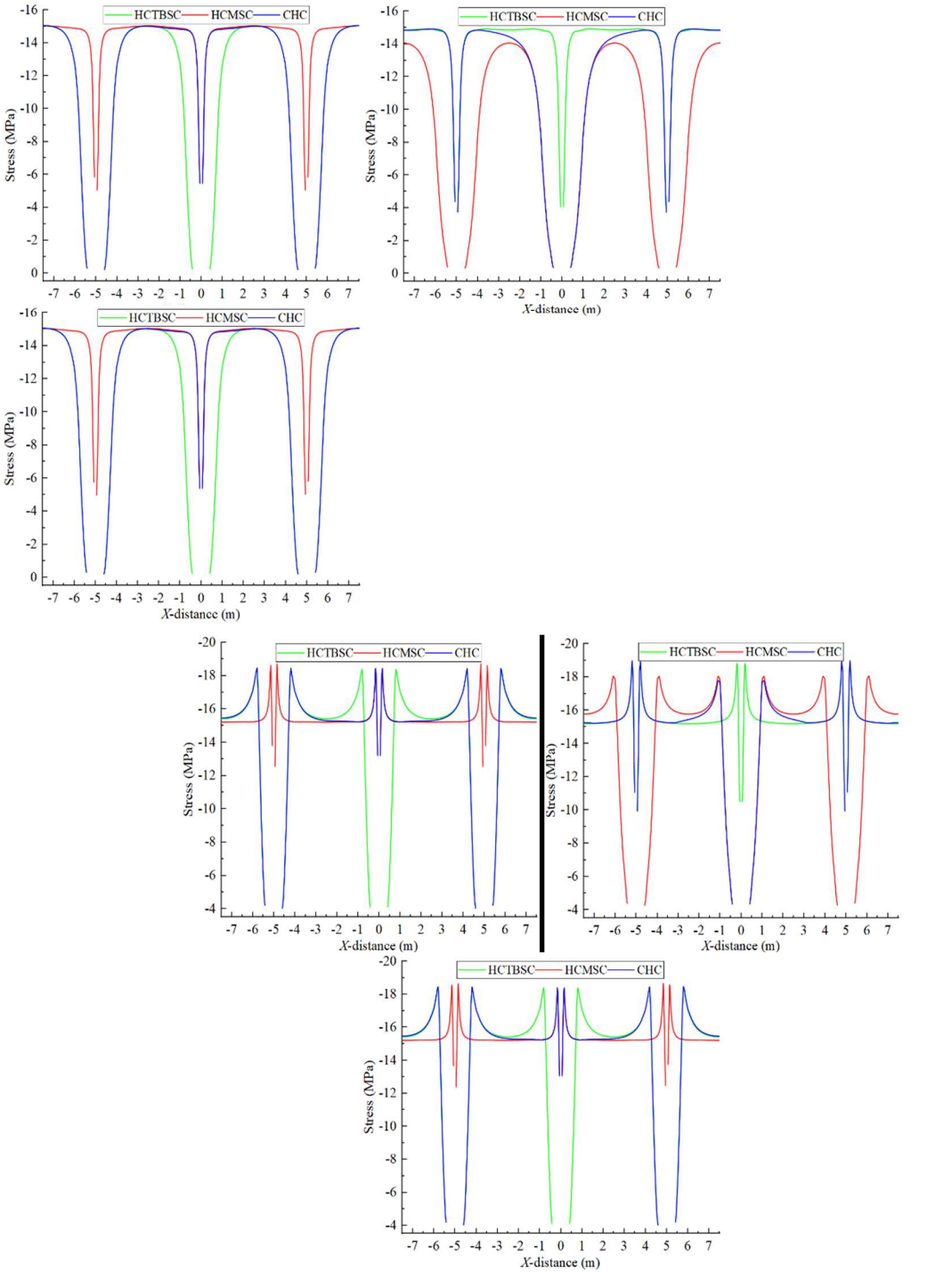

h = 4.95 m h = 7.47 m h = 9.99 m

(a) R=0.4 m

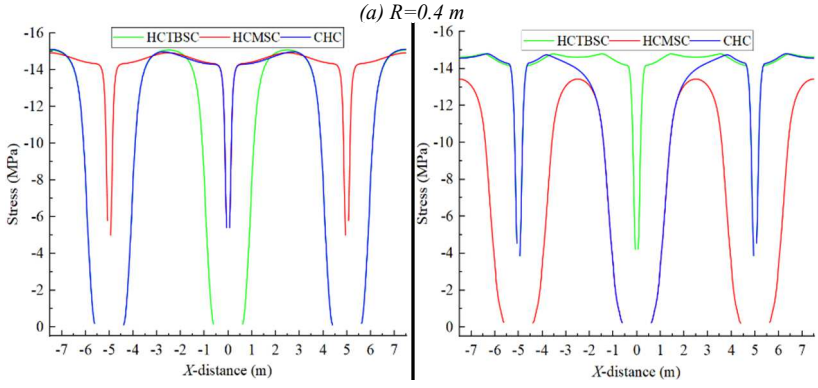

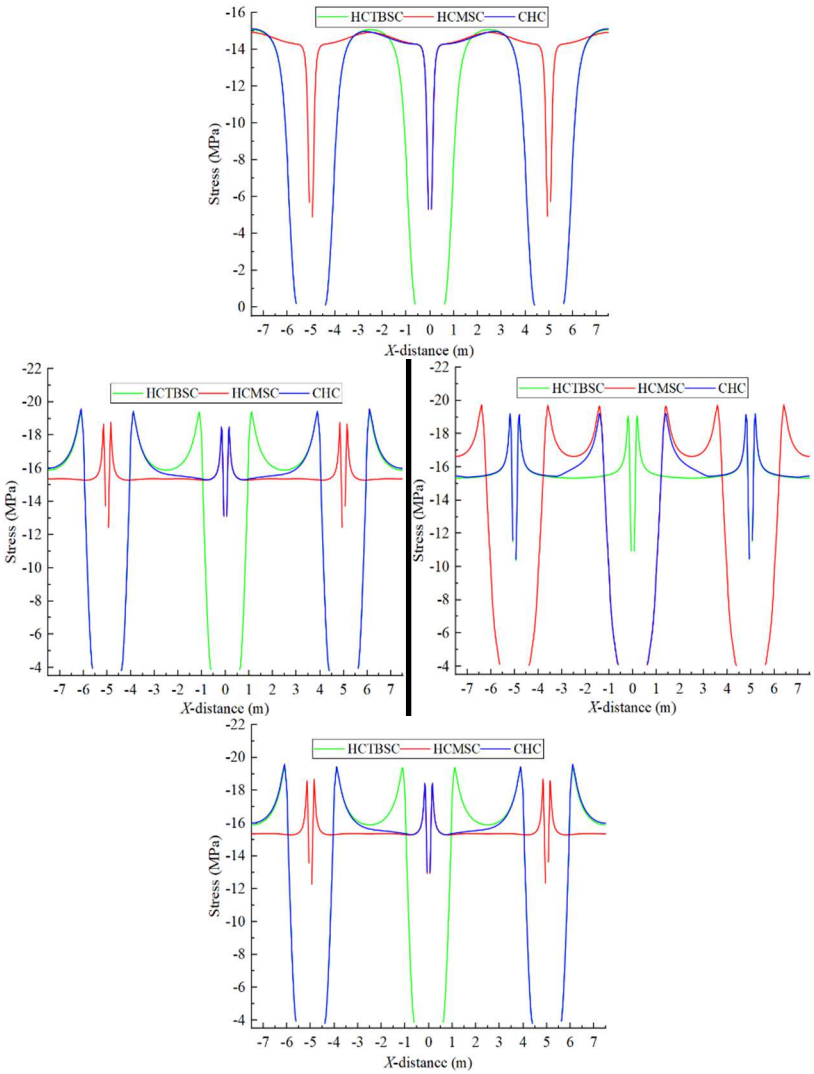

h = 4.95 m h = 7.47 m h = 9.99 m

(b) R=0.6m

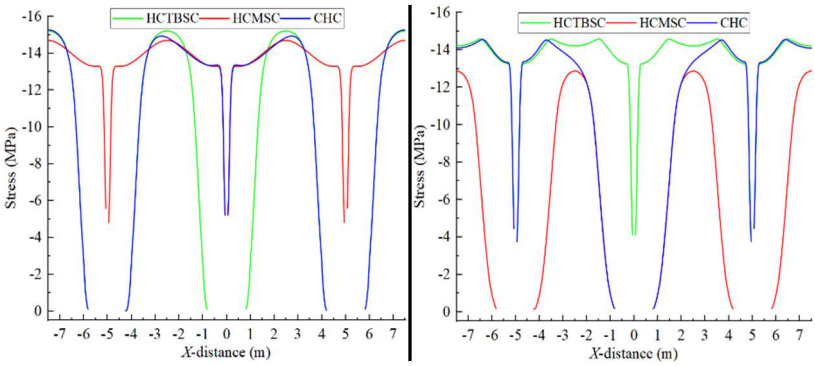

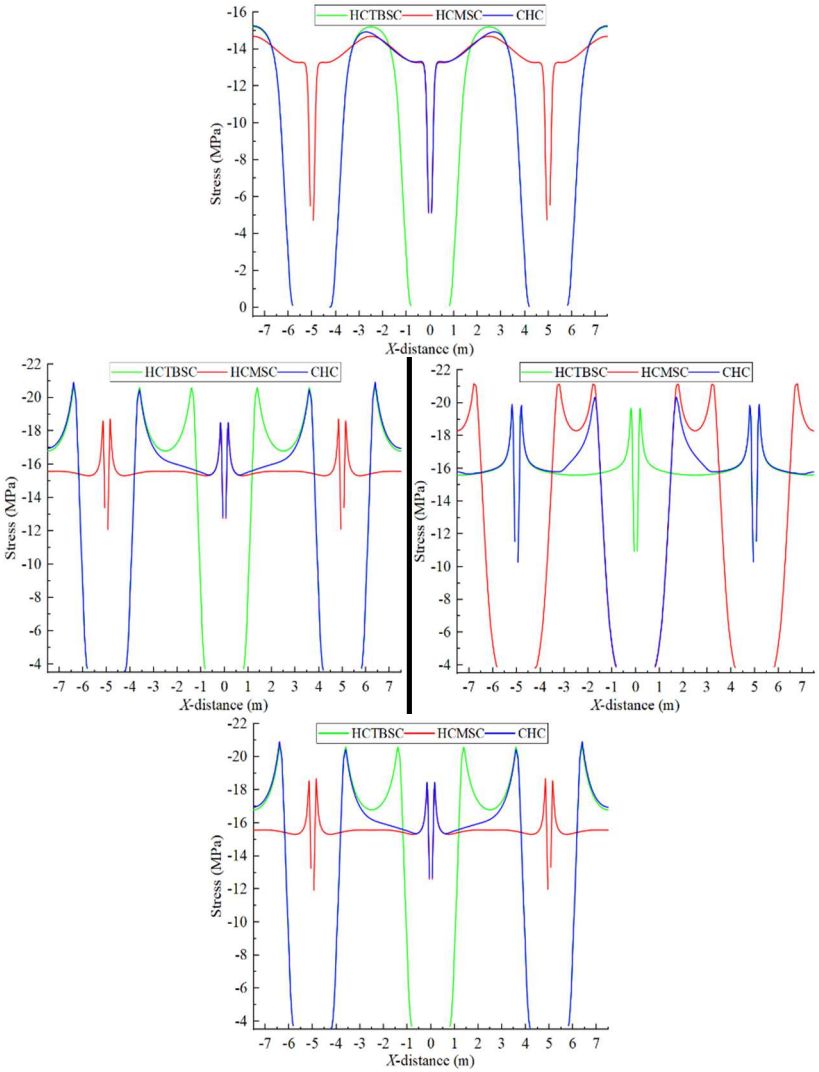

h = 4.95 m *h* = 7.47 m *h* = 9.99 m

(c) R=0.8m

Fig. 12. Stress allocation curve with different cavitation distribution forms.

Field trial verification analysis

Comparing the consistency of gas drainage. A total of 16 boreholes were selected from the 40 boreholes in the test area, including 8 HCTBSC, 4 conventional boreholes, and 4 cavitation boreholes in the borehole interval hydraulic cavitation area near the trial area. The gas consistency monitoring data of 16 boreholes from the 5th to the 12th week after gas drainage were analyzed by a line graph comparing the productiveness of gas drainage, as shown in Figs. 13 and 14.

In Fig. 13, the gas consistency of the trial borehole is basically approximate to the cavitation borehole in interval hydraulic cavitation; the overall gas drainage consistency of the trial borehole is slightly higher than the cavitation borehole in interval hydraulic cavitation. While the gas drainage consistency decay rate of the boreholes is basically the same for the two technical measures, the two coal stratum decompression techniques can basically ensure that the gas drainage consistency of the borehole is still around 60% at the end of the third month. Therefore, regarding the cavitation borehole, the impact of the two-seam decompression techniques on the productiveness of gas drainage is not significant.

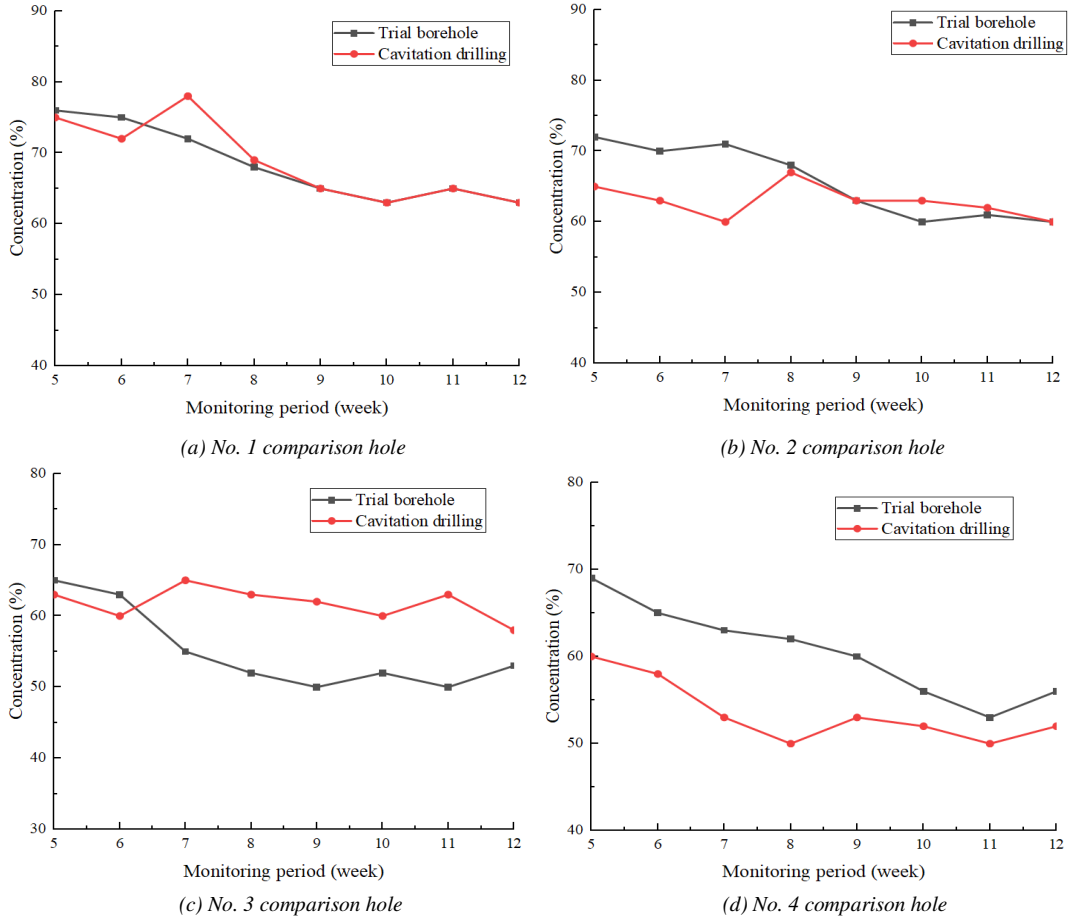

(a) No. 1 comparison hole *(b) No. 2 comparison hole*

(c) No. 3 comparison hole *(d) No. 4 comparison hole*

Fig. 13. Comparison of gas consistency between trial holes and cavitation holes.

In Fig. 14, the gas consistency of the trial borehole is apparently better than the conventional borehole in the interval-type hydraulic cavitation borehole; the gas consistency decay rate between them is not much different. So, the productiveness of gas drainage from the trial borehole is better than the conventional borehole in the interval-type hydraulic cavitation borehole.

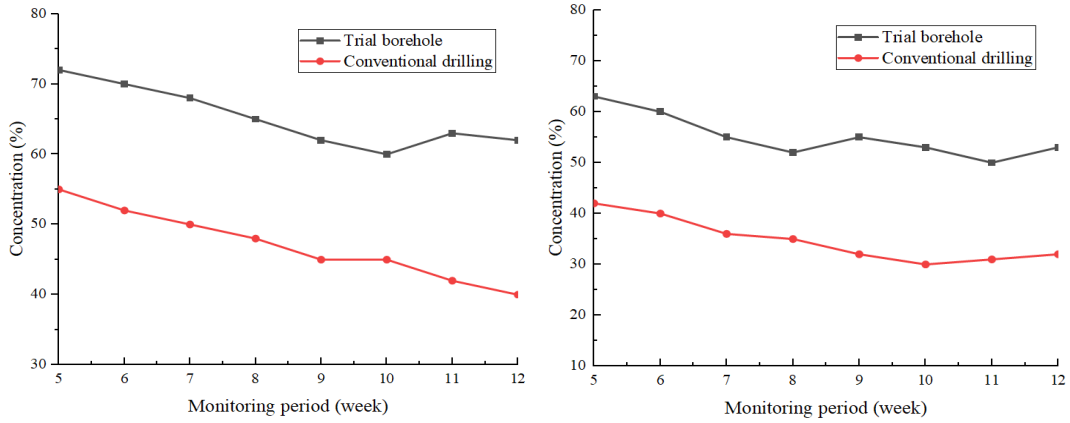

(a) No. 1 comparison hole *(b) No. 2 comparison hole*

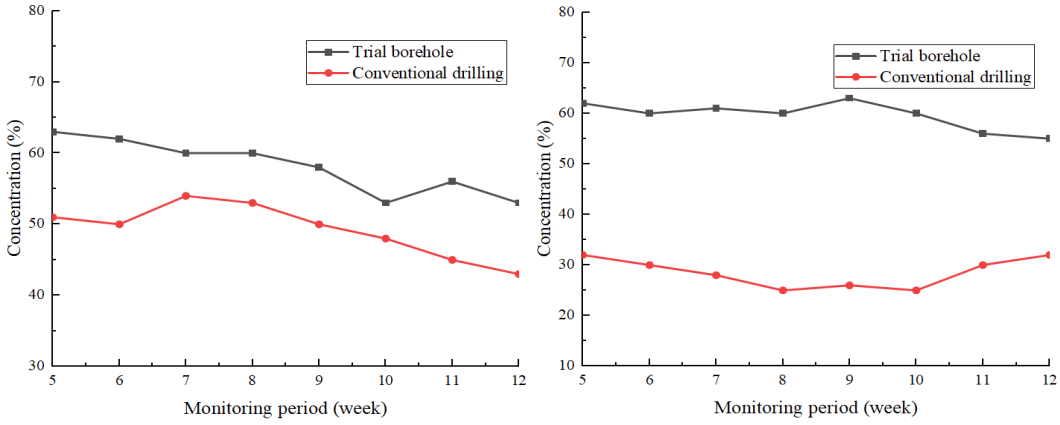

(c) No. 3 comparison hole *(d) No. 4 comparison hole*

Fig. 14. Comparison of gas consistency between trial holes and cavitation holes

In Figs. 13 and 14, the productiveness of gas drainage by HCTBSC is significantly higher than the interval hydraulic cavitation in the borehole. Therefore, the use of HCTBSC in the Wuyang coal mine can increase the productiveness of gas drainage, which can help to quickly eliminate the risk of protrusion in high gas areas and realize rapid roadway excavation.

In Fig. 15, the gas drainage mixing amount of the trial borehole is only slightly higher than the interval-type hydraulic cavitation borehole, but the pure gas drainage amount of the trial borehole is significantly higher than the interval-type hydraulic cavitation borehole, which is 1.5 times than the pure gas drainage amount of the interval type cavitation borehole, the gas drainage of the 3# coal of Wuyang coal mine by using HCTBSC can better augment the productiveness of gas drainage, shorten the gas drainage time of Wuyang coal gas drainage standard time.

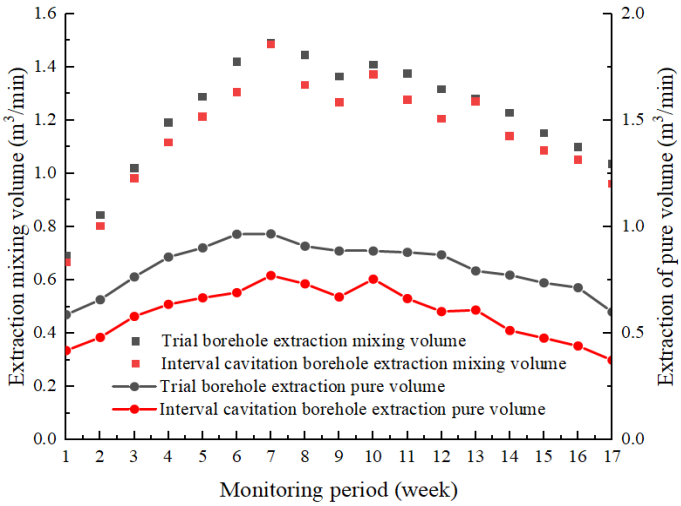

Fig. 15. Comparison of gas extraction volume.

Conclusions

To solve the problem of the low effectiveness of hydraulic cavitation construction, forming the stress concentration areas in coal after cavitation, the technology of HCTBSC was proposed in the Wuyang coal mine. Using a research approach combining theoretical analysis, numerical simulation, and field test, the stress allocation was analyzed in coal after cavitation to compare the stress in coal under different cavitation radii and different cavitation distribution forms. The main conclusions are obtained as follows:

(1) The ESR of HCTBSC, HCMSC, and CHC is related to the cavitation radius and the distance of the borehole. When the distance of the borehole is certain, as the increment of cavitation radius, the ESR progressively increases.

(2) When the cavitation radius is different, with the increase of cavitation radius, the minimum principal stress relief range and the maximum principal stress value in the coal increase continuously. When the cavitation distribution form is different, the DSR of the three cavitation distribution forms is mainly concentrated around the

cavitation chamber; with the increase of cavitation radius, the DSR extends to all orientations in the coal with the cavitation chamber as the center.

(3) The gas extraction data in the field test proclaim that HCTBSC improves the consistency and pure volume of gas drainage, proving the applicability of the technology in the Wuyang coal mine.

Only the field test of HCTBSC was conducted; the comparison of the field test of HCMSC and CHC was not conducted. Therefore, the subsequent research will compare the coal permeability and gas seepage for the three hydraulic cavitation means mentioned in the study.

Reference

Ahamed, M. A. A., Perera, M. S. A., Elsworth, D., Ranjith, P. G., Matthai, S. K. M., Dong-yin, L. (2021). Effective application of proppants during the hydraulic fracturing of coal seam gas reservoirs: Implications from laboratory testings of propped and unpropped coal fractures. Fuel, 304. pp. 121394. DOI: 10.1016/j.fuel.2021.121394.

Black, D.J. (2019). Review of coal and gas outburst in Australian underground coal mines. International Journal of Mining Science and Technology, 29(6). pp. 815-824. DOI: 10.1016/j.ijmst.2019.01.007.

Cao, Z.Y., Wang, E.Y., He, X.Q., Wang, H., Liu, Q.L., Zhang, G.H., Luo, F., Wang, C. and Xu, Y.L. (2021). Effect evaluation of pressure relief and gas drainage of hydraulic punching in short-distance coal seam group with the risk of outburst. Journal of Mining & Safety Engineering, 38(3). pp. 634-642. DOI: 10.13545/j.cnki.jmse.2020.0206.

Chen, Y.B., Li, D.Q., Wang, S.R., Zou, Z.S. and Rabe, M. (2022). Study on mechanism of pressure relief and permeability enhancement in soft-hard composite coal seam by directional hydraulic flushing technology. Acta Montanistica Slovaca, 27(2). pp. 522-536. DOI: 10.46544/AMS.v27i2.18.

Cheng, X., Zhao, G.M., Li, Y.M., Meng, X.R., Dong, C.L. and Xu, W.S. (2018). Study on relief-pressure antireflective effect and gas extraction technology for mining soft rock protective seam. Journal of Mining & Safety Engineering, 35(5). pp. 1045-1053. DOI: 10.13545/j.cnki.jmse.2018.05.023.

Godec, D., Brnadić, V. and Breški, T. (2021). Optimisation of mould design for injection moulding-numerical approach. Technical Journal, 15(2). pp. 258-266. DOI: 10.31803/tg-20210531204548.

Gu, B.F. and Wu, Y.L. (2021). Research and Application of Hydraulic Punching Pressure Relief Antireflection Mechanism in Deep "Three-Soft" Outburst Coal seam. Shock and Vibration, 2021. pp. 7241538. DOI: 10.1155/2021/7241538.

Hao, F.C., Sun, L.J. and Liu, M.J. (2014). Research on boreholes space optimization of hydraulic flushing considering press relief and gas drainage effect. Journal of Mining & Safety Engineering, 31(5). pp. 756-763. DOI: 10.13545/j.issn1673-3363.2014.05.015.

Huang, B.X., Cheng, Q.Y., Chen, S.L. and Zhang, T. (2013). Study of coal seam outburst mitigation by deep hole hydro-fracturing and shallow hole methane drainage. Journal of China University of Mining & Technology, 42(5). pp. 701-711. DOI: 10.13247/j.cnki.jcumt.2013.05.001.

Ivakhnenko, O., Aimukhan, A., Kenshimova, A., Mullagaliyev, F., Akbarov, E., Mullagaliyeva, L., Kabirova, S., Almukhametov, A. (2017). Advances in coalbed methane reservoirs integrated characterization and hydraulic fracturing for improved gas recovery in Karaganda Coal Basin, Kazakhstan. Energy Procedia, 125. pp. 477-485. DOI: 10.1016/j.egypro.2017.08.161.

Jeffrey, R. G., Chen, Z. R., Zhang, X., Bunger, A. P., Mills, K. W. (2015). Measurement and Analysis of Full-Scale Hydraulic Fracture Initiation and Reorientation. Rock Mechanics and Rock Engineering, 48(6). pp. 2497-2512. DOI: 10.1007/s00603-015-0846-3.

Jiang, F.X., Liu, Y., Liu, J., Zhang, M., Du, J.P., Sun, W.S. and Zhang, W.P. (2019). Pressure-releasing mechanism of local protective layer in coal seam with rock burst. Chinese Journal of Geotechnical Engineering, 41(2). pp. 368-375. DOI: 10.11779/CJGE201902016.

Kataoka, M.N., Ferreira, M.A. and de Cresce, El.A.L.H. (2017). Nonlinear FE analysis of slab-beam-column connection in precast concrete structures. Engineering structures, 143. pp. 306-315. DOI: 10.1016/j.engstruct.2017.04.028.

Kim, D. and Jeong, S. (2021). Estimation of the excavation damage zone in TBM tunnel using large deformation FE analysis. Geomechanics and Engineering, 24(4). pp. 323-335. DOI: 10.12989/gae.2021.24.4.323.

Kolomiets, L.V., Aniskin, A., Daschenko, A., Lymarenko, A.M. Boriak, K.F. (2021). Application of numerical methods for research of construction design of fastener fractures. Technical Journal, 15(2). pp. 178-183. DOI: 10.31803/tg-20191023141118.

Li, D.Q. (2014). Underground hydraulic mining of thin sub-layer as protective coal seam in coal mines. International Journal of Rock Mechanics and Mining Sciences, 67. pp. 145-154. DOI: 10.1016/j.ijrmms.2014.01.014.

Li, G. and Teng, J.F. (2021). Research and optimization of gas extraction by crossing-seam boreholes from floor roadway. Geofluids, 2021. pp. 7499012. DOI: 10.1155/2021/7499012.

Li, P., Zhang, X.D. and Li, H. (2021). Technology of coupled permeability enhancement of hydraulic punching and deep-hole pre-splitting blasting in a "three-soft" coal seam. Materials and Technology, 55(1). pp. 89-96. DOI: 10.17222/mit.2020.075.

Li, Y.Q., Yang, K., Qin, R.X. and Yu, Y. (2020). Technical system and prospect of safe and efficient mining of coal and gas outburst coal seam. Coal Science and Technology, 48(3). pp. 167-173. DOI: 10.13199/j.cnki.cst.2020.03.020.

Liu, X., Li, Y., Xuan, D.Q., Hu, S.X., Jing, T.X. and Xu, S. (2021). Numerical simulation and test of gas drainage with water jet layered pressure relief and permeability enhancement in soft coal seam. Coal Geology & Exploration, 49(2). pp. 54-61. DOI: 61.1155.p.20210323.1640.006.

Liu, H.B., Cheng, Y.P., Song, J.C., Shang, Z.J. and Wang, L. (2009). Pressure relief, gas drainage and deformation effects on an overlying coal seam induced by drilling an extra-thin protective coal seam. Mining Science and Technology (China), 19(6). pp. 724-729. DOI: 10.1016/S1674-5264(09)60132-0.

Liu, H. B., Liu, H. and Cheng, Y.P. (2014). The elimination of coal and gas outburst disasters by ultrathin protective seam drilling combined with stress-relief gas drainage in Xinggong coalfield. Journal of Natural Gas Science and Engineering, 21. pp. 837-844. DOI: 10.1016/j.jngse.2014.10.022.

Long, L.J., Liu, D.Y., Wang, D. and Li, J. (2021). Mechanical properties of sandstone subjected to coupling of temperature-seepage-stress. DYNA, 96(3). pp. 309-315. DOI: 10.6036/10055.

Lu, Y.Y., Huang, S., Ge, Z.L., Zhou, Z., Liu, W.C. and Guan, Y.R. (2022). Research progress and strategic thinking of coal mine water jet technology to enhance coal permeability in China. Journal of China Coal Society, 47(9). pp. 3189-3211. DOI: 10.13225/j.cnki.jccs.SS22.0602.

Garagash, I. A., Osiptsov, A. A., Boronin, S. A. (2019). Dynamic bridging of proppant particles in a hydraulic fracture. International Journal of Engineering Science, 135. pp. 86-101. DOI: 10.1016/j.ijengsci.2018.11.004.

Pezdevsek, M., Kevorkijan, L. and Bilus, I. (2022). Cavitation erosion modelling-comparison of two solid angle projection approaches. International Journal of Simulation Modelling, 21(2). pp. 249-260. DOI: 10.2507/IJSIMM21-2-600.

Si, G.Y., Durucan, S., Shi, J.Q., Korre, A. and Cao, W.Z. (2019). Parametric analysis of slotting operation induced failure zones to stimulate low permeability coal seam. Rock Mechanics and Rock Engineering, 52(1). pp. 163-182. DOI: 10.1007/s00603-018-1579-x.

Soleimani, F., Si, G.Y., Roshan, H. and Zhang, Z.Y. (2023). Numerical modelling of coal and gas outburst initiation using energy balance principles. Fuel, 334. pp. 126687. DOI: 10.1016/j.fuel.2022.126687.

Vasyliev, D. (2019). Parameters of interaction of a hydro impulse device with a coalseam during its loosening. E3S Web of Conferences, 109. pp. 00110. DOI: 10.1051/e3sconf/201910900110.

Wang, S.R., Li, J.T., Li, D.Q., Chen, Y.B. and Zhang, J.Y. (2021a). Analysis on collapse prevention and support for bedding borehole in soft coal. Journal of Engineering Science and Technology Review, 14(4). pp. 146-152. DOI: 10.25103/jestr.144.18.

Wang, S.R., Wang, Y.H., Wang, Z.L., Gong, J. and Li, C.L. (2021b). Anchoring performances analysis of tension-torsion grouted anchor cable under free and non-free rotation conditions. DYNA, 96(2). pp. 166-172. DOI: 10.6036/9985.

Wang, S.R., Zhao, J.Q., Wu, X.G., Yang, J.H. and Liu, A. (2021c). Meso-scale simulations of lightweight aggregate concrete under impact loading. International Journal of Simulation Modelling, 20(2). pp. 291-302. DOI: 10.2507/IJSIMM20-2-558.

Wang, W., Wang, G., Zhao, W., Wang, L., Feng, Z.K., Cui, R. and Du, F. (2022). Numerical assessment of the pressure relief effect of the hydraulic punching cavitation technique in a soft coal seam. Geomechanics and Geophysics for Geo-Energy and Geo-Resources, 30(8). pp. 367. DOI: 10.1007/s40948-022-00339-9.

Wei, G.M., Wen, H., Deng, J., Li, Z.B., Fan, S.X., Lei, C.K., Liu, M.Y. and Ren, L.F. (2020). Enhanced coalbed permeability and methane recovery via hydraulic slotting combined with liquid CO_2 injection. Process Safety and Environmental Protection, 147. pp. 234-244. DOI: 10.1016/j.psep.2020.08.033.

Xie, H.P., Zhou, H.W., Xue, D.J., Wang, H.W., Zhang, R. and Gao, F. (2012). Research and consideration on deep coal mining and critical mining depth. Journal of China Coal Society, 37(4). pp. 535-542. DOI: 10.13225/j.cnki.jccs.2012.04.011.

Xu, Y.P., Wang, L.G. Bhattacharyya, S., Peng, X.S. and Chen, X.J. (2021). Improving safety by further increasing the permeability of coal seam using air cannons after hydraulic punching. Arabian Journal of Geosciences, 14. pp. 2126. DOI: 10.1007/s12517-021-08511-3.

Yan, H., Zhang, J.X., Ju, Y., Pu, H., Zhang, Q. and Zhang, S. (2018). Fracture development rules controlled by backfill body's compression ratio and gas drainage technology under upper protective layer mining. Journal of Mining & Safety Engineering, 35(6). pp. 1262-1268. DOI: 10.13545/j.cnki.jmse.2018.06.024.

Yang, Y.B. and Zhou, Z. (2022). Strength and fracture characteristics of coal rock disturbed by protective layer mining under graded cyclic loading. Journal of Zhejiang University (Engineering Science), 56(12). pp. 2445-2453. DOI: 10.3785/j.issn.1008-973X.2022.12.013.

Yao, B.H., Ma, Q.Q., Wei, J.P., Ma, J.H. and Cai, D.L. (2016). Effect of protective coal seam mining and gas extraction on gas transport in a coal seam. International Journal of Mining Science and Technology, 26(4). pp. 637-643. DOI: 10.1016/j.ijmst.2016.05.016.

Yuan, L., Lin, B.Q. and Yang, W. (2015). Research progress and development direction of gas control with mine hydraulic technology in China coal mine. Coal Science and Technology, 43(1). pp. 45-49. DOI: 10.13199/j.cnki.cst.2015.01.011.

Zberovskyi, V., Sofiiskyi, K., Stasevych, R., Pazynych, A., Pinka, J. and Sidorova, M. (2020). The results of monitoring of hydroimpulsive disintegration of outburst-prone coal seam using ZUA-98 system. E3S Web of Conferences, 168. pp. 00068. DOI: 10.1051/e3sconf/202016800068.